Springer

Journal of Mechanical Science and Technology 23 (2009) 3049~3058

Journal of Mechanical Science and Technology

www.springerlink.com/content/1738-494x
DOI 10.1007/s12206-009-0821-6

Identification of the beat characteristics and damping ratios of the Hwacheon World Peace Bell using wavelet transform †

Sung Yong Park[1], Won Tae Jeong[1], Seockhyun Kim[2,*] and Yeon June Kang[1]

[1]*Department of Mechanical and Aerospace Engineering, Seoul National University, Seoul, 151-744, Korea*
[2]*Division of Mechanical and Mechatronics Engineering, Kangwon National University, Kangwon-Do,200-701, Korea*

(Manuscript Received April 14, 2009; Revised July 23, 2009; Accepted July 30, 2009)

Abstract

In this paper, a new measurement technique is proposed to identify the beat characteristics and modal damping ratios of a Korean bell in the casting field. The beat response caused by the mutual interference of mode pair with very close doublet frequency is unique feature of the Korean bell and should be accurately measured in order to quantitatively estimate the bell sound. However, the conventional method based on a filtering concept such as the Fourier transform has difficulty in extracting the beat frequencies and modal damping ratios because the method should individually decompose the measured signal into each mode. The aim of this paper is to propose an effective measurement method to identify the beat frequencies, mode pairs and modal damping ratios using the continuous wavelet transform in a real striking condition. The proposed method is verified with the Hwacheon World Peace Bell cast in the year 2008, which is the largest bell in Korea. In the future, the proposed method can be applicable to the casting field of the Korean bell to effectively estimate its beat characteristics and damping characteristics.

***Keywords*:** Beat characteristics; Mode pair; Modal damping ratio; Continuous wavelet transform; Hwacheon World Peace Bell

1. Introduction

The beating response of the Korean bell is created by the mutual interference of mode pair with very close doublet frequency. The Korean bell consists of a main axisymmetric shell with decorative sculptures and carved figures on the surface. The sculptures, carved figures and casting irregularities introduce asymmetry into the bell. As a result, mode pairs with doublet frequency are generated in the circumferential direction [1]. When a certain mode pair is equally excited by the external impact, then the beat response of the mode pair is generated. The Korean bell has a breathing-like beat which is a unique feature compared with western bells. For the breathing-like beat, a clear beat and proper beat period are desired for the liveliness of the Korean bell sound. Recently, a study on the beat control was carried out in order to improve the beat characteristic condition [2, 3]. To identify and control the beat characteristics of the Korean bell, it is inevitably necessary to decompose the mode pair into each mode from the measured signal. In the conventional method, the low and high mode consisting of the mode pair were individually excited, and then the mode shape, beat frequency and modal damping were individually extracted by the measured signal. Also, when the measured signal includes the components of the low and high mode of a certain mode pair, the modal properties of the bell are measured through the filtering method [4]. In this case, it is very difficult to individually excite the two modes with the very close natural frequency. Also, the filtering process also needs to work hard in decomposing the measured signal into each mode.

† This paper was recommended for publication in revised form by Associate Editor Eung-Soo Shin

*Corresponding author. Tel.: +82 33 250 6372
E-mail address: seock@kangwon.ac.kr

In this study, an effective measurement method is proposed to identify the beat frequencies, mode pairs and modal damping ratios in a real striking condition. The proposed method was applied to the Hwacheon World Peace Bell cast in the year 2008, which is the largest bell in Korea, weighing 37.5 ton. The proposed method using the continuous wavelet transform [5-8] can identify the beat frequencies, mode shapes and modal damping ratios for the several tones of the bell at a time. The beat frequencies and beat period of each mode pair are obtained by using the continuous wavelet transform (CWT) based on the Gabor wavelet. Also, the modal damping ratios associated with the time duration of the beat response are also identified by the CWT. When using the CWT on a given signal, the optimal shape of the Gabor wavelet used as the mother wavelet is determined by employing the Shannon entropy cost function on the normalized wavelet modulus.

This paper is organized in the following way. In section 2, the mode decoupling process of the multi-degree of freedom system is explained using the CWT. After that, the analytical beat characteristics of each mode are examined using a slightly asymmetric cylindrical shell, which can analyze the beat characteristics of the Korean bell. Next, we identify the mode shapes of the Hwacheon World Peace Bell. Finally, the beat characteristics and modal damping ratios of the bell are identified by using the continuous wavelet transform.

2. Theoretical background of the continuous wavelet transform

The continuous wavelet transform $W_\psi x(u,s)$ [9] of an L_2 -based signal $x(t)$ is defined by

$$W_\psi x(u,s) = \int_{-\infty}^{\infty} x(t)\psi^*_{u,s}(t)dt, \tag{1}$$

where

$$\psi_{u,s}(t) = \frac{1}{\sqrt{s}}\psi\left(\frac{t-u}{s}\right), \ s>0, \ u \in \mathrm{R}. \tag{2}$$

Here, $\psi^*(t)$ is the complex conjugate of the mother wavelet $\psi(t)$, which is dilated with a scale parameter s related to the frequency and translated by translation parameter u localizing the wavelet in the time-domain. The CWT represents the convolution sum between a given signal $x(t)$ and a scaled mother wavelet $\psi(t)$.

Many mother wavelets have been employed in taking the CWT of a given signal. In analyzing the frequency evolution of a given signal, the CWT should use analytic wavelets such as the Gabor wavelet which has the smallest Heigenberg box [9]. The Gabor wavelet $\psi(t)$ can be constructed with a frequency modulation of a real and symmetric Gaussian window $g(t)$:

$$\psi(t) = g(t)\mathrm{e}^{\mathrm{i}\eta t} \tag{3}$$

with

$$g(t) = \frac{1}{\left(\sigma^2\pi\right)^{1/4}}\mathrm{e}^{\left(\frac{-t^2}{2\sigma^2}\right)}, \tag{4}$$

where η is the center frequency of $\Psi(\omega)$ and σ is the measure of time spread of $\psi(t)$. The shape of the Gabor wavelet is controlled by the combination between η and σ. The product of η and σ is called as the Gabor shaping factor $G_s = \sigma\eta$ [5]. Because the time-frequency resolution of the CWT based on the Gabor wavelet is determined by the Gabor shaping factor, the optimal shape of the Gabor wavelet should be selected [5, 6].

In Eq. (3), the dilated version of the Fourier transform for the Gabor wavelet is defined by

$$\Psi(s\omega) = \left(4\pi\sigma^2\right)^{1/4}\mathrm{e}^{\left\{\frac{-\sigma^2}{2}(s\omega-\eta)^2\right\}}. \tag{5}$$

$\Psi(s\omega)$ of Eq. (5) has a maximum value at the center frequency of the mother wavelet, i.e., $s\omega = \eta$. This implies that the Gabor wavelet can be considered as a band-pass filter, because it has a fast decay at the frequency ranges outside of the center frequency.

3. Estimation of the beat characteristics and damping ratios using the CWT

3.1 The CWT of mono- and multi-spectral signals

Consider the wavelet transform for $x(t) = A(t)\cos(\phi(t))$ of the Single Degree of Freedom (SDOF) system where $A(t)$ and $\phi(t)$ are an amplitude and a time-varying phase, respectively. If $x(t)$ is assumed to be an asymptotic signal, an analytic function of $x(t)$ is

$$x_a(t) = A(t)\mathrm{e}^{\mathrm{i}\phi(t)}. \tag{6}$$

The wavelet transform based on the Gabor wavelet can

be obtained as

$$W_\psi x(u,s) = \frac{1}{2}\langle x_a(t), \psi_{u,s}(t)\rangle$$
$$= \frac{\sqrt{s}}{2} A(u) e^{i\phi(u)} \left\{ G(\eta - s\phi'(u)) + \varepsilon\left(u, \frac{\eta}{s}\right)\right\}, \quad (7)$$

where $G(\omega)$ is the Fourier transform of the Gaussian window function $g(t)$. Using $\Psi(\omega) = G(\omega - \eta)$, $G(\eta - s\phi'(u))$ in Eq. (7) becomes $\Psi^*(s\phi'(u))$. If $A(t)$ and $\phi'(t)$ have small variation over the support of $\psi_{u,s}(t)$ and if $\phi'(u)$ is larger than $\Delta\omega_\psi / s$ where $\Delta\omega_\psi$ is frequency bandwidth of the mother wavelet, the corrective term $\varepsilon(u, \eta/s)$ can be neglected. Therefore, Eq. (7) can be finally approximated as

$$W_\psi x(u,s) \cong \frac{\sqrt{s}}{2} A(u) e^{i\phi(u)} \Psi^*(s\phi'(u)). \quad (8)$$

Since $\Psi(s\omega)$ has a maximum value at $s\omega = \eta$, the absolute wavelet transform $|W_\psi x(u,s)|$ is maximum at $s(u)\phi'(u) = \eta$, which are the wavelet ridge points. The wavelet ridges are a collection of corresponding points $(u, \phi'(u))$, at which the normalized energy density called the wavelet scalogram becomes a local maximum at each time.

Consider that $x(t)$ is the response of the multi-degree of freedom (MDOF) system. The response of the *N*-DOF system can be expressed as a summation of the response of the SDOF system as follows:

$$x(t) = \sum_{k=1}^{N} x_k(t) = \sum_{k=1}^{N} A_k(t) e^{i\phi_k(t)},$$
$$k = 1, 2, ..., i-1, i, i+1, ..., N, \quad (9)$$

where $A_k(t)$ and $\phi_k(t)$ are an amplitude and a time-varying phase of $x_k(t)$, respectively.

Since the CWT is a linear transformation of a given signal, the CWT of the signal with the multi-spectral components is given by the summation of that of SDOF signal:

$$W_\psi x(u,s) = W_\psi \left\{ \sum_{k=1}^{N} x_k(u,s) \right\}$$
$$\cong \sum_{k=1}^{N} \frac{\sqrt{s}}{2} A_k(u) e^{i\phi_k(u)} \Psi^*(s_k \phi_k'(u)). \quad (10)$$

In Eq. (10), if we choose the optimal Gabor shaping factor in order to have sufficient frequency resolution, we can decouple the close natural modes. In other words, because the mother wavelet function has compact support in the frequency and time domains, the wavelet transform at the scale parameter s_i associated with the *i*th dynamic mode can only provide a relevant contribution. On the other hand, at a scale parameter not associated with the *i*th dynamic mode, the wavelet transform cannot provide any contribution:

$$\Psi^*(s_k \phi_k'(u)) = 0$$
$$\text{for } k = 1, 2, ..., i-1, i+1, ..., N. \quad (11)$$

Thus, the wavelet transform of the MDOF system can be decoupled into each mode of the SDOF system:

$$W_\psi x_i(u, s_i) = \frac{\sqrt{s_i}}{2} A_i(u) e^{i\phi_i(u)} \Psi^*(s_i \phi_i'(u)). \quad (12)$$

Finally, the mode decoupling procedure of the MDOF system is effectively accomplished by the CWT.

3.2 Extracting the beat characteristics and damping ratios of bell type structures

Bell type structures, including the Korean bell, can be modeled as a slightly asymmetric cylindrical shell or circular ring. By the impulse response analysis, the beat response of each (m, n) mode in a slightly asymmetric cylindrical shell is given by [4]

$$u_{3mn}(x^*, \theta, t)$$
$$= e^{-\zeta_{mnu}\omega_{mnu}t} \left\{ \cos n(\theta^* - \phi_{mnL}) \cos n(\theta - \phi_{mnL}) \sin(\omega_{mnL} t) \right.$$
$$\left. + \cos n(\theta^* - \phi_{mnH}) \cos n(\theta - \phi_{mnH}) \sin(\omega_{mnH} t) \right\}, \quad (13)$$

where ω_{mnH} and ω_{mnL} are the natural frequency of the high mode and the natural frequency of the low mode, respectively. Two mode components have slightly different frequency values by the slight asymmetry. Subscripts m and n mean the mode sequence of the longitudinal direction and the mode sequence of the radial direction in the Korean bell, respectively. θ^* is the position of the striking point. φ_{mnH} and φ_{mnL} are the position of the anti-node for the high mode and the position of the anti-node for the low mode, respectively. The phase difference between the low and high mode in a certain mode

pair is given by

$$\phi_{mnH} = \phi_{mnL} + \frac{\pi}{2n}, \quad n = 2, 3, 4, ..., \infty . \tag{14}$$

The average values of frequency and damping are used as follows, since these values for each mode pair are almost the same:

$$\omega_{mna} = (\omega_{mnL} + \omega_{mnH})/2$$
$$\text{and} \quad \zeta_{mna} = (\zeta_{mnL} + \zeta_{mnH})/2 . \tag{15}$$

By using Eq. (12), the CWT for a certain mode (m, n) of a slightly asymmetric cylindrical shell, as shown in Eq. (13), is given by

$$W_\psi u_{3mn}(u,s) = W_\psi u_{3mnL}(u,s) + W_\psi u_{3mnH}(u,s), \tag{16}$$

where

$$W_\psi u_{3mnL}(u,s) = \frac{C_{mnL}}{2}\sqrt{s}\, e^{-\zeta_{mna}\omega_{mna}u}\Psi^*(s\omega_{mnL})e^{i\omega_{mnL}u}, \tag{17}$$

$$W_\psi u_{3mnH}(u,s) = \frac{C_{mnH}}{2}\sqrt{s}\, e^{-\zeta_{mna}\omega_{mna}u}\Psi^*(s\omega_{mnH})e^{i\omega_{mnH}u}, \tag{18}$$

$$C_{mnL} = \cos n(\theta^* - \phi_{mnL})\cos n(\theta - \phi_{mnL}),$$
$$C_{mnH} = \cos n(\theta^* - \phi_{mnH})\cos n(\theta - \phi_{mnH}) . \tag{19a,b}$$

Here, C_{mnL} and C_{mnH} are the contribution factor of the low mode $(m, n)_L$ and the contribution factor of the high mode $(m, n)_H$ contributing to the beat response, respectively.

Since the dilated mother wavelet function $\Psi(s_{\omega_{mna}}\omega)$ is a symmetric function at the center frequency η on the ω-axis, $\Psi^*(s_{\omega_{mna}}\omega_{mnL})$ is equal to $\Psi^*(s_{\omega_{mna}}\omega_{mnH})$ where $s_{\omega_{mna}}$ is the scale parameter corresponding to the average frequency ω_{mna} of the low and high mode. Thus, at the average frequency ω_{mna}, Eq. (16) becomes as follows:

$$\begin{aligned} &W_\psi u_{3mn}(u, s_{\omega_{mna}}) \\ &= \frac{\sqrt{s_{\omega_{mna}}}}{2} e^{-\zeta_{mna}\omega_{mna}u}\Psi^*(s_{\omega_{mna}}\omega_{mnL}) \\ &\quad \{C_{mnL}e^{i\omega_{mnL}u} + C_{mnH}e^{i\omega_{mnH}u}\}, \\ &= \frac{\sqrt{s_{\omega_{mna}}}}{2} e^{-\zeta_{mna}\omega_{mna}u}\Psi^*(s_{\omega_{mna}}\omega_{mnL})R_{mn}e^{i\Theta_{mn}} \end{aligned} \tag{20}$$

where

$$R_{mn} = \sqrt{C_{mnL}^2 + C_{mnH}^2 + 2C_{mnL}C_{mnH}\cos\{(\omega_{mnH} - \omega_{mnL})u\}}, \tag{21}$$

$$\Theta_{mn} = \tan^{-1}\left(\frac{C_{mnL}\sin\omega_{mnL}u + C_{mnH}\sin\omega_{mnH}u}{C_{mnL}\cos\omega_{mnL}u + C_{mnH}\cos\omega_{mnH}u}\right). \tag{22}$$

To obtain the modulus of the wavelet transform, we must take the absolute value for $W_\psi u_{3mn}(u, s_{\omega_{mna}})$:

$$\left|W_\psi u_{3mn}(u, s_{\omega_{mna}})\right| = \frac{\sqrt{s_{\omega_{mna}}}}{2} e^{-\zeta_{mna}\omega_{mna}u}\left|\Psi^*(s_{\omega_{mna}}\omega_{mnL})R_{mn}\right|, \tag{23}$$

In Eq. (23), the envelope of the wavelet modulus $\left|W_\psi u_{3mnL}(u, s_{\omega_{mna}})\right|$ at ω_{mna} is a function of $\cos\{(\omega_{mnH} - \omega_{mnL})u\}$. The period of the amplitude-modulated envelope in the wavelet modulus indicates the beat period of the (m, n) beating mode:

$$T_{mn} = \frac{4\pi}{\omega_{mnH} - \omega_{mnL}}. \tag{24}$$

To extract the damping ratio of the (m, n) mode associated with the beat response, we take a semi-logarithm of the wavelet modulus $\left|W_\psi u_{3mn}(u, s_{\omega_{mna}})\right|$ to obtain the following:

$$\begin{aligned} &\ln\left|W_\psi u_{3mn}(u, s_{\omega_{mna}})\right| \\ &= -\zeta_{mna}\omega_{mna}u + \ln\left\{\frac{\sqrt{s_{\omega_{mna}}}}{2}\left|\Psi^*(s_{\omega_{mna}}\omega_{mnL})R_{mn}\right|\right\}, \end{aligned} \tag{25}$$

The damping ratios of a given signal $u_{3mn}(t)$ can be identified by calculating the slope of the straight line having a translation parameter u as an independent variable on the semi-logarithm of the wavelet modulus.

If C_{mnL} is equal to C_{mnH}, i.e., an in-phase contribution of a low $(m, n)_L$ and high mode $(m, n)_H$ to a beat response of the (m, n) mode, Eq. (20) can be rewritten as

$$\begin{aligned} &W_\psi u_{3mn}(u, s_{\omega_{mna}}) \\ &= C_{mnL}\sqrt{s_{\omega_{mna}}}\, e^{-\zeta_{mna}\omega_{mna}u}\Psi^*(s_{\omega_{mna}}\omega_{mnL})\cos\alpha_{mn}\, e^{i\beta_{mn}}, \end{aligned} \tag{26}$$

where

$$\alpha_{mn} = (\omega_{mnH} - \omega_{mnL})u/2$$
$$\text{and} \quad \beta_{mn} = (\omega_{mnH} + \omega_{mnL})u/2 . \tag{27a,b}$$

If C_{mnL} is equal to $-C_{mnH}$, i.e., an out-of-phase contribution of a low $(m, n)_L$ and high mode $(m, n)_H$ to beat response of the (m, n) mode, Eq. (20) can be rewritten as

$$W_\psi u_{3mn}\left(u, s_{\omega_{mna}}\right) = -\mathrm{i}C_{mnL}\sqrt{s_{\omega_{mna}}}\,\mathrm{e}^{-\zeta_{mna}\omega_{mna}u}\Psi^*\left(s_{\omega_{mna}}\omega_{mnL}\right)\sin\alpha_{mn}\mathrm{e}^{\mathrm{i}\beta_{mn}}. \quad (28)$$

As can be seen in Eq. (26), when the contribution of the low and high mode contributing to the beat response is the same, the wavelet modulus shows the function of $\cos\alpha_{mn}$ at the average frequency between the low and high mode. On the other hand, as can be seen in Eq. (28), if the contribution of the low and high mode contributing to the beat response is out-of-phase, the wavelet modulus is the function of $\sin\alpha_{mn}$. In the same manner, the period of the envelope in the wavelet modulus is $T_{mn} = 4\pi/\left(\omega_{mnH} - \omega_{mnL}\right)$.

In Eqs. (26) and (28), the argument of $W_\psi u_{3mn}\left(u, s_{\omega_{mna}}\right)$ is given by

$$arg\left\{W_\psi u_{3mn}\left(u, s_{\omega_{mna}}\right)\right\} = \left(\omega_{mnH} + \omega_{mnL}\right)u/2. \quad (29)$$

If we take a derivative with respect to the translation parameter for Eq. (29), the average value of the low and high frequency for the (m, n) mode can be obtained as

$$\omega_{mna} = \frac{d}{du}arg\left\{W_\psi u_{3mn}\left(u, s_{\omega_{mna}}\right)\right\} = \left(\omega_{mnH} + \omega_{mnL}\right)/2. \quad (30)$$

Finally, the natural frequencies of the low mode ω_{mnL} and high mode ω_{mnH} for the (m, n) mode can be obtained from Eqs. (24) and (30), respectively.

$$\omega_{mnL} = \omega_{mna} - \frac{2\pi}{T_{mn}} \quad \text{and} \quad \omega_{mnH} = \omega_{mna} + \frac{2\pi}{T_{mn}}. \quad (31a,b)$$

4. Experimental results and discussion

4.1 Vibration modes of the Hwacheon World Peace Bell

As shown in Fig. 1 and Table 1, because the Hwacheon World Peace Bell is a very massive structure, it is difficult to generate vibration modes using a general commercialized impact hammer or exciter. In this research, a loud speaker and a frequency generating system are used to resonate the low mode $(m, n)_L$ and high mode $(m, n)_H$ individually. For the effective resonance of each mode, the loud speaker for the low frequency range was set at the anti-node position of each mode and the bell was accurately excited by each natural frequency without producing any beat. Comparing the 24-point signals with the reference signal at point 23 makes it possible to determine the magnitude and the phase of the acceleration at each position in Fig. 2(b). The modal amplitude A_{ij} and modal phase Φ_{ij} of the *i*th mode shape for the bell are obtained by [8]

$$A_{ij} = \left|\frac{W_\psi^j x(u, s_i)}{W_\psi^R x(u, s_i)}\right|, \quad \Phi_{ij} = \arg\left(\frac{W_\psi^j x(u, s_i)}{W_\psi^R x(u, s_i)}\right), \quad (32)$$

where $W_\psi^j(u, s_i)$ is the wavelet transform of the measured signal at *j*th position and $W_\psi^R(u, s_i)$ represents the wavelet transform of the reference signal for *i*th mode sequence.

Using the wavelet technique of Eq. (32), we measured the mode pairs for the hum mode $(0, 2)$ and fundamental mode $(0, 3)$. In Fig. 3, the vibration mode pairs for $(0, 2)$ and $(0, 3)$ modes are plotted on the circumference at the positions with 15° increments and along the contour of the bell. In Fig. 3 (a), the phase difference between $(0, 2)_L$ mode and $(0, 2)_H$ mode is almost 45° on the circumferential direction. In Table 2, the node position and anti-node

Table 1. Dimensions of the Hwacheon World Peace Bell.

Parts	D_u	D_l	D_d	H_b
Dimensions [mm]	1,890	2,745	565	3,620
Parts	H_d	H_e	H_s	T_b
Dimensions [mm]	910	1,020	80	247

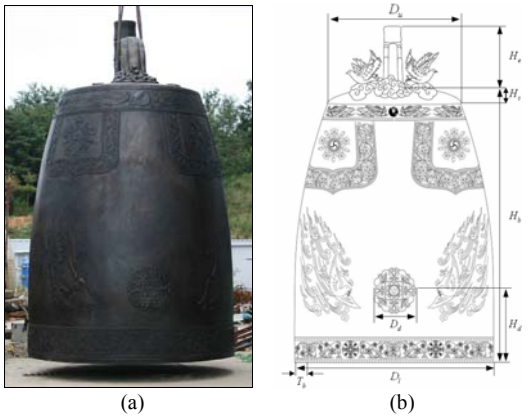

(a) (b)

Fig. 1. (a) The Hwacheon World Peace Bell and (b) its dimensions.

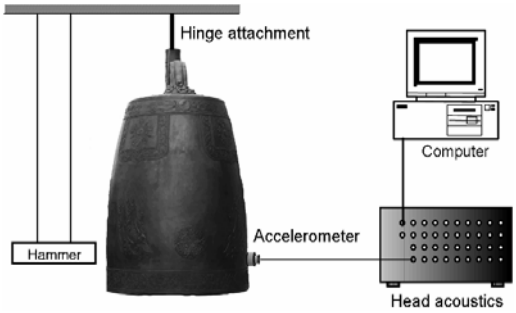

(a) Experimental setup

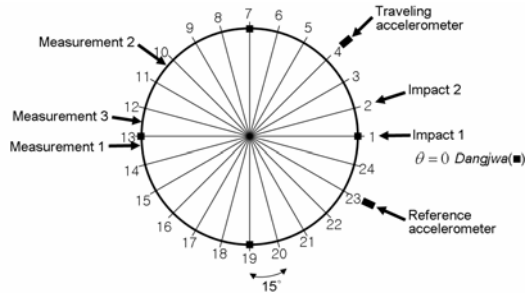

(b) The position of impact and measurement

Fig. 2. (a) Experimental setup for measuring vibration and (b) the positions of impact and measurement (bottom view).

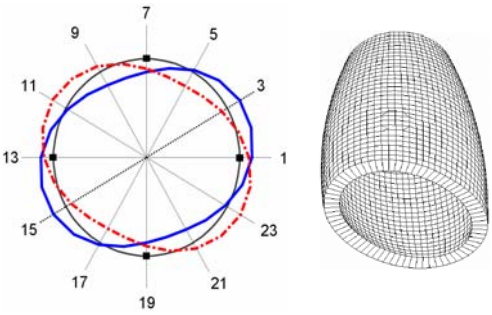

(a) *Mode* (0, 2): (i) Experiment, (ii) FEM

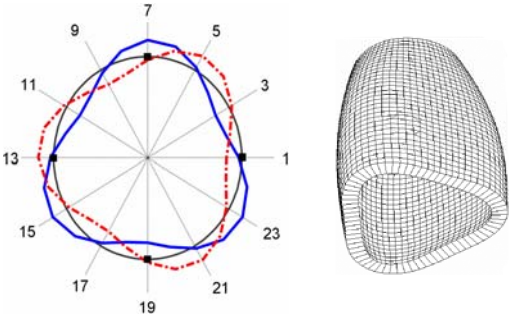

(b) *Mode* (0, 3): (i) Experiment, (ii) FEM

Fig. 3. Vibration modes of the Hwacheon World Peace Bell by the experiment and finite element analysis: (a) *Mode* (0, 2), (b) *Mode* (0, 3). (——) Low mode; (- · -) High mode.

position of the $(0, 2)_L$ mode are almost -26.25° and 18.75° around the impact position $(\theta = 0^\circ)$, respectively. Therefore, the present striking position excites almost equally both $(0, 2)_L$ mode and $(0, 2)_H$ mode. This configuration of the mode pair and striking position satisfies the condition for a strong beat in the hum mode $(0, 2)$. In Table 2 and Fig. 3(b), the node position and anti-node position of the $(0, 3)_L$ mode are almost -3.75° and 26.25° around the impact position $(\theta = 0^\circ)$, respectively. The phase difference between $(0, 3)_L$ mode and $(0, 3)_H$ mode is almost 30° on the circumferential direction. In the present striking position, because the present striking position strongly excites the $(0, 3)_H$ mode, a clear beat for fundamental mode $(0, 3)$ is not generated. For three-dimensional mode shapes of the bell, the finite element analysis using the commercial program ANSYS was carried out for the bell. The mode shapes of the bell obtained from the finite element analysis are shown in Fig. 3. The results are very similar to those by the experiments.

4.2 Beat characteristics and damping ratio of the Hwacheon World Peace Bell

The proposed continuous wavelet technique was applied to identify the beat characteristics and damping ratios of the Hwacheon World Peace Bell. The dimensions of the bell and experimental setup for impact testing are described in Table 1 and in Fig. 2, respectively. The external force of the bell for impact testing was excited by a wooden hammer called *Dangmok*, and acceleration signals from the bell were measured using PCB type uniaxial accelerometers. Impact signals of the bell were gathered by Head acoustic signal analyzer system. Since the amplitude and the phase between the low and high mode contributing to beating response of (m, n) mode in the bell are different from one position to another, the determination of measurement point and striking position is very important in accurately measuring the beat response of each mode. In this paper, the striking position of the impact hammer and the measurement position by the accelerometer are illustrated in Fig. 2(b).

First, we chose Impact 1 as the first striking position and Measurement 1 as the first measurement position. The temporal response under the impact testing is shown in Fig. 4. Before performing the CWT of the measured signal, the optimal Gabor shap-

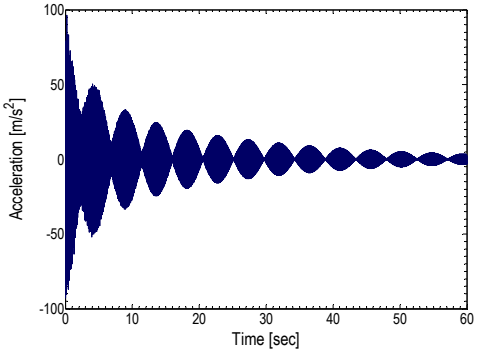

Fig. 4. The beating response under the impact testing.

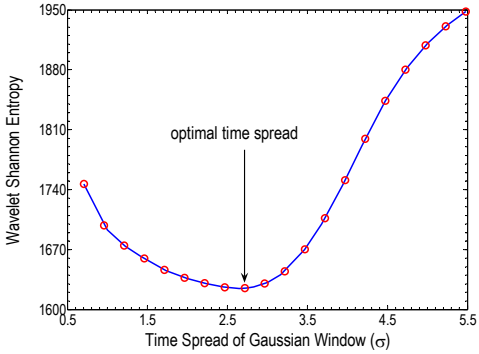

Fig. 5. The wavelet Shannon entropy of the measured signal.

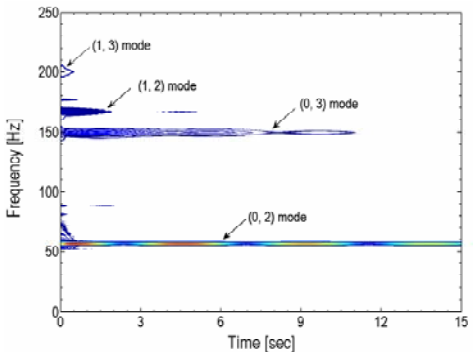

Fig. 6. The wavelet modulus of the measured signal. The striking position and measurement position are Impact 1 and Measurement 1, respectively.

ing factor was obtained by using the Shannon wavelet entropy [6]. In this simulation, we selected the center frequency to be 12π, and then the optimal time spread σ of the Gaussian window was determined to be $\sqrt{15/2}$, as shown in Fig. 5. Using the optimal Gabor shaping factor G_{sopt}, we carried out the CWT on the measured signal, as shown in Fig. 6. The wavelet modulus contour in Fig. 6 has one beating mode,

Table 2. Positions of the node and anti-node for hum and fundamental modes.

Mode $(2, 0)_L$		*Mode* $(2, 0)_H$	
Node	Anti-node	Node	Anti-node
-26.25°	18.75°	18.75°	63.75°
Mode $(3, 0)_L$		*Mode* $(3, 0)_H$	
Node	Anti-node	Node	Anti-node
-3.75°	26.25°	26.25°	56.25°

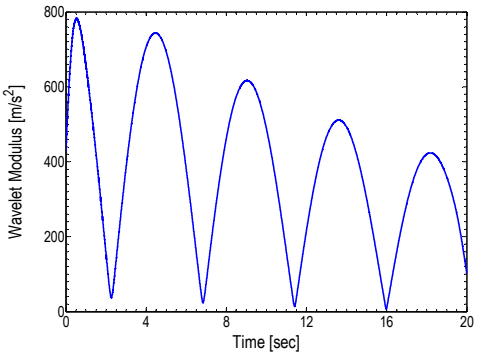

(a) Wavelet modulus of (0, 2) mode

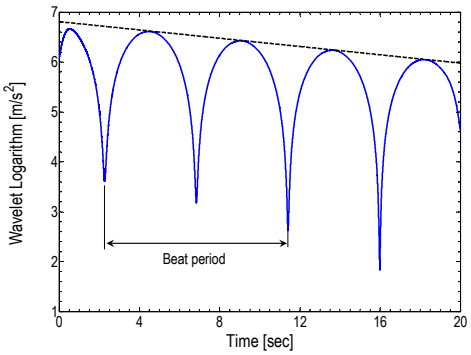

(b) Wavelet semi-logarithm of (0, 2) mode

Fig. 7. The wavelet modulus of (0, 2) mode and its semi-logarithm for the measured signal. The striking position and measurement position are Impact 1 and Measurement 1, respectively.

which is the $(0, 2)$ mode, and three exponential decay modes, which are the $(0, 3)$ mode, $(1, 2)$ mode and $(1, 3)$ mode. The wavelet modulus was extracted at the first average frequency, and then we took the semi-logarithm on the wavelet modulus for estimating the beat periods, natural frequencies and modal damping ratios of the low and high mode. As shown in Fig. 7(a), because the contribution between the low and high mode contributing to the $(0, 2)$ beating response is in-phase at the position of Measurement 1, the wavelet modulus for the (0, 2) beating

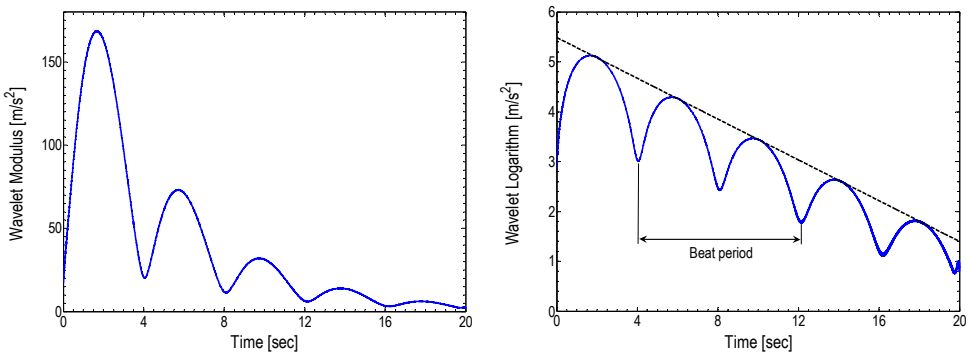

(a) Wavelet modulus of (0, 3) mode (b) Wavelet semi-logarithm of (0, 3) mode

Fig. 8. The wavelet modulus of (0, 3) mode and its semi-logarithm for the measured signal. The striking position and measurement position are Impact 1 and Measurement 2, respectively.

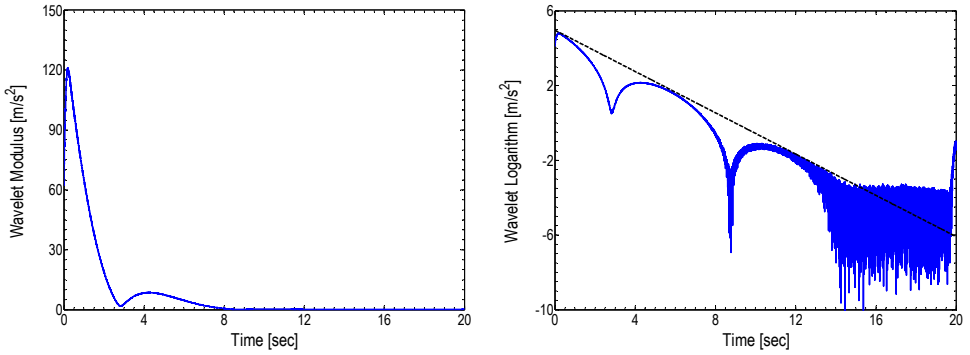

(a) Wavelet modulus of (1, 2) mode (b) Wavelet semi-logarithm of (1, 2) mode

Fig. 9. The wavelet modulus of (1, 2) mode and its semi-logarithm for the measured signal. The striking position and measurement position are Impact 2 and Measurement 3, respectively.

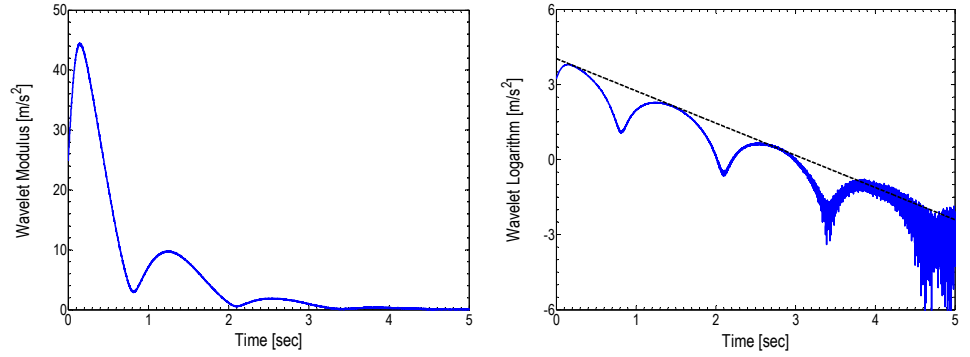

(a) Wavelet modulus of (1, 3) mode (b) Wavelet semi-logarithm of (1, 3) mode

Fig. 10. The wavelet modulus of (1, 3) mode and its semi-logarithm for the measured signal. The striking position and measurement position are Impact 1 and Measurement 2, respectively.

mode shows a cosine wave. From the semi-logarithm of the wavelet modulus for $(0, 2)$ mode, we obtained beat period, modal damping ratio and natural frequencies of the low and high mode, as listed in Table 3.

As shown in Fig. 3(b), because the position of Impact 1 and Measurement 1 is close to the node position of $(0, 3)_L$ mode, the response at Measurement 1 does not contain the beat characteristics of $(0, 3)$ mode. To identify the beat characteristics of $(0, 3)$

Table 3. Estimated beat periods, damping ratios and natural frequencies of the measured signal.

Mode No.	Averaged frequency [Hz]	Beat period [sec]	Damping ratio (ζ_{mna})
1	56.63	9.14	0.00012
2	149.07	7.91	0.00022
3	165.06	11.72	0.00054
4	202.36	2.58	0.00104

Mode No.	Mode sequence (m, n)	Natural frequency using CWT [Hz]	Natural frequency using FEM [Hz]
1	$(0, 2)_L$	56.52	56.42
	$(0, 2)_H$	56.74	56.72
2	$(0, 3)_L$	148.94	148.80
	$(0, 3)_H$	149.19	150.12
3	$(1, 2)_L$	164.98	169.84
	$(1, 2)_H$	165.15	170.64
4	$(1, 3)_L$	201.97	204.35
	$(1, 3)_H$	202.75	205.62

mode, we chose Impact 1 as the first striking position and Measurement 2 as the first measurement position. Because the contribution between the low and high mode contributing to the $(0, 3)$ beating response is out-of-phase at the position of Measurement 2, the wavelet modulus for the $(0, 3)$ beating mode is a sine wave, as shown in Fig. 8.

As shown in Fig. 6, the wavelet modulus contour of the response measured at Measurement 1 has the exponential decay response characteristics for the third and fourth beating mode. For this reason, we cannot obtain the beat characteristics such as beat period and modal damping ratio at the third and fourth beating mode. To obtain the beat characteristics and modal damping ratio of the third beating mode, we chose Impact 2 for the excitation of the bell and Measurement 3 for measuring the beating response. Also, we chose Impact 1 for the excitation of the bell and Measurement 2 for measuring the fourth beating mode. Similarly, we estimated the damping ratios, natural frequencies and beat periods at the third and fourth average frequencies on the wavelet modulus contour and its semi-logarithm, as shown in Figs. 9 and 10.

5. Conclusion

We have effectively identified the beat characteristics and modal damping ratios of the Hwacheon World Peace Bell using the CWT. The modal decoupling procedure of a beating signal was easily carried out using the CWT based on the Gabor wavelet. Before taking the CWT for a beating signal, the optimal shape of the Gabor wavelet was determined by employing the Shannon entropy cost function. The beat characteristics and modal damping ratios of the bell were obtained from the wavelet modulus at each mode and its semi-logarithm. The beat period and beat frequency of the hum mode in the Hwacheon World Peace Bell are 9.14 s and 57 Hz, while those of the fundamental mode are 7.91 s and 149 Hz, respectively. The current striking position enables a clear beat to be well produced in hum mode, while the beat in fundamental mode is not well generated because the striking position is close to the node position of the low mode.

Acknowledgments

This work was supported by Institute of Advanced Machinery and Design at Seoul National University and Brain Korea 21 Project of the Ministry of Education, Korea. The authors thank Sungjongsa Co., LTD. in Korea that supported the experiment on the Hwacheon World Peace Bell.

References

[1] S. H. Kim, W. Soedel and J. M. Lee, Analysis of the beating response of bell type structures, *J. Sound Vib.* 173 (4) (1994) 517-536.

[2] H. G. Park, S. H. Kim and Y. J. Kang, Analytical method of beat tuning in a slightly asymmetric ring, *J. Mech. Science Tech.* 21 (8) (2007) 1226-1234.

[3] H. G. Park, Y. J. Kang and S. H. Kim, Dual mode tuning strategy of a slightly asymmetric ring, *J. Acoust. Soc. Am.* 123 (3) (2008) 1383-1391.

[4] S. H. Kim, C. W. Lee and J. M. Lee, Beat characteristics and beat maps of the King Seong-deok Divine Bell, *J. Sound Vib.* 281 (2005) 21-44.

[5] Y. Y. Kim and E. H. Kim, A new damage detection method based on a wavelet transform, *Proceedings of 18th IMAC* (2000) 1207-1212.

[6] S. Y. Park, B. U. Jeon, J. M. Lee and Y. H. Cho, Measurement of low-frequency wave propagation in a railway contact wire with dispersive character-

istics using wavelet transform, *Key Eng. Mater.* 321-323 (2006) 1609-1615.
[7] J. Lardies and S. Gouttebroze, Identification of modal parameters using the wavelet transform, *Int. J. Mech. Science.* 44 (2002) 2263-2283.
[8] Thien-Phu Le and Pierre Argoul, Continuous wavelet transform for modal identification using free decay response, *J. Sound Vib.* 277 (2004) 73-100.
[9] S. Mallat, *A Wavelet Tour of Signal Processing*, Academic press, New York, USA, (1998).

Sung Yong Park received his B.S. degree in Mechanical Engineering from Myongji University (Yongin, Korea) in 2003. After completing the B.S. degree, he received Ph.D. degree from the School of Mechanical and Aerospace Engineering at Seoul National University (Seoul, Korea) in 2009. His main research areas are the coupling analysis of the vibro-acoustic coupled system, the modal parameter estimation of the mechanical system using the continuous wavelet transform. Also, he has been particularly interested in the vibration analysis and design of the Korean bell. He is now working as a researcher of HDD storage division in Samsung Electronics.

Seockhyun Kim received the B.S. and the Ph.D. degree in Mechanical Engineering from Seoul National University (Seoul, Korea) in 1980 and 1987 respectively. In 1988, he joined the faculty of Kangwon National University, where he is currently a professor in the school of Mechatronics Engineering. His main research areas include Korean bells, vibration analysis of the high speed railway vehicle, vibration and noise analysis of the wind turbine, the coupling analysis of the vibro-acoustic coupled system and so on. Also, he is now working as a member of the Editorial Board in the Journal of Mechanical Science and Technology, and a vice-chairman of the Society of Korean bell (Korea).